Published in final edited form as:
J Comp Neurol. 2003 September 22; 464(3): 356–370.

Connexin29 and Connexin32 at Oligodendrocyte and Astrocyte Gap Junctions and in Myelin of the Mouse Central Nervous System

James I. Nagy[1,*], **Andrei V. Ionescu**[1], **Bruce D. Lynn**[1], and **John E. Rash**[2]

1 *Department of Physiology, Faculty of Medicine, University of Manitoba, Winnipeg, Manitoba R3E 3J7, Canada*

2 *Department of Anatomy and Neurobiology and Program in Molecular, Cellular and Integrative Neurosciences, Colorado State University, Fort Collins, Colorado 80523*

Abstract

The cellular localization, relation to other glial connexins (Cx30, Cx32, and Cx43), and developmental expression of Cx29 were investigated in the mouse central nervous system (CNS) with an anti-Cx29 antibody. Cx29 was enriched in subcellular fractions of myelin, and immunofluorescence for Cx29 was localized to oligodendrocytes and myelinated fibers throughout the brain and spinal cord. Oligodendrocyte somata displayed minute Cx29-immunopositive puncta around their periphery and intracellularly. In developing brain, Cx29 levels increased during the first few postnatal weeks and were highest in the adult brain. Immunofluorescence labeling for Cx29 in oligodendrocyte somata was intense at young ages and was dramatically shifted in localization primarily to myelinated fibers in mature CNS. Labeling for Cx32 also was localized to oligodendrocyte somata and myelin and absent in Cx32 knockout mice. Cx29 and Cx32 were minimally colocalized on oligodendrocytes somata and partly colocalized along myelinated fibers. At gap junctions on oligodendrocyte somata, Cx43/Cx32 and Cx30/Cx32 were strongly associated, but there was minimal association of Cx29 and Cx43. Cx32 was very sparsely associated with astrocytic connexins along myelinated fibers. With Cx26, Cx30, and Cx43 expressed in astrocytes and Cx29, Cx32, and Cx47 expressed in oligodendrocytes, the number of connexins localized to gap junctions of glial cells is increased to six. The results suggested that Cx29 in mature CNS contributes minimally to gap junctional intercellular communication in oligodendrocyte cell bodies but rather is targeted to myelin, where it, with Cx32, may contribute to connexin-mediated communication between adjacent layers of uncompacted myelin.

Indexing terms

brain; glia; antibodies; intercellular communication; confocal microscopy; Schmidt-Lanterman incisures

Cells in the central nervous system (CNS) communicate directly via gap junctions at close appositions between plasma membranes, thereby providing channels for movement of ions and small molecules from cell to cell. It appears that virtually every neural cell type in the brain has the capacity for gap junctional intercellular communication (GJIC), and evidence for several levels of complexity in this process is beginning to emerge. Each cell type exhibits

*Correspondence to: James I. Nagy, Department of Physiology, Faculty of Medicine, University of Manitoba, 730 William Ave, Winnipeg, Manitoba R3E 3J7, Canada. E-mail: nagyji@ms.umanitoba.ca.

Grant sponsor: Canadian Institutes of Health Research (J.I.N.); Grant sponsor: National Institutes of Health (J.E.R); Grant number: NS44010; Grant number: NS44395; Grant number: NS38121.

Published online the week of August 4, 2003 in Wiley InterScience (www.interscience.wiley.com).

selectivity with respect to cellular coupling partners and to connexin (Cx) coupling partners (Nagy and Rash, 2000; Nagy et al., 2003a). Extensive homologous coupling occurs between astrocytes (A/A gap junctions), and widespread heterologous coupling also occurs between astrocytes and oligodendrocytes (A/O gap junctions), but little if any homologous coupling occurs between oligodendrocytes (Mugnaini, 1986; Rash et al., 1997, 2000; Nagy et al., 2003a). In addition, vast numbers of gap junctions have been reported to connect not only astrocyte processes of different cells but also those of the same cell, resulting in extensive autocellular coupling formed by autologous or reflexive gap junctions (Wolburg and Rohlmann, 1995; Nagy and Rash, 2000). At least 10 members of the family of connexin proteins that form gap junctions in mammalian tissues are expressed in the CNS, and individual cells and gap junctions often contain two or more different connexins (Nagy et al., 1999; Severs, 1999; Nagy and Dermietzel, 2000; Nagy and Rash, 2000). It is now established that A/A junctions contain Cx26, Cx30, and Cx43, and that A/O junctions contain these connexins on the astrocyte side and Cx32 on the oligodendrocyte side (Dermietzel et al., 1989; Yamamoto et al., 1990a,b; Scherer et al., 1995; Wolburg and Rohlmann, 1995; Dahl et al., 1996; Li et al., 1997; Ochalski et al., 1997; Kunzelmann et al., 1999; Nagy et al., 1999; Rash et al., 2000, 2001).

Multiple connexin expression in each pair of gap junctionally coupled cells introduces the possibility of heterotypic channel formation between different connexins, some heterotypic combinations of which are functionally permissive, whereas others are not (White and Bruzzone, 1996). This suggests a diversity of functional GJIC depending on the connexins expressed by cells and the differential permeability of channels formed by the different connexins (Veenstra, 1996). The organization of heterologous gap junctions of oligodendrocytes with astrocytes in the CNS is not yet clear. Even though Cx32 and Cx43 are reported to be nonpermissive for gap junction channel formation, Cx43, Cx30, and Cx26 are nevertheless incorporated into gap junction plaques on the astrocyte side of A/O junctions on oligodendrocyte somata (Ochalski et al., 1997; Nagy et al., 1997, 1999, 2001; Rash et al., 2001). The presence of Cx43 at A/O junctions suggests that it may couple to other connexins in oligodendrocytes. Coupling partner candidates include Cx29 and Cx47, both of which are highly expressed in neural tissues and localized to oligodendrocytes (Sohl et al., 2001; Altevogt et al., 2002; Li et al., 2002; Nagy et al., 2003a,b). In addition, Cx32 in the CNS is densely localized nearly continuously along myelinated fibers (Li et al., 1997), thus differing from Cx32 localization in myelin of the peripheral nerve, where it is highly concentrated at the nodes of Ranvier and Schmidt-Lanterman incisures. In CNS myelin, Cx32 may form gap junctions with astrocytic processes that abut myelinated fibers, as has been described to occur in the CNS (Waxman and Black, 1984; Ochalski et al., 1997), or it may form autologous or reflexive gap junctions between successive layers of cytoplasmic pockets to allow radial GJIC, as has been proposed to occur in the peripheral nerve (Balice-Gordon et al., 1998).

In the present study, the expression and cellular localization of Cx29 in adult and developing mouse CNSs were investigated by western blotting, light microscopy, and confocal laser scanning immunofluorescence by using a well characterized anti-Cx29 antibody (Li et al., 2002). In addition, the cellular localizations of Cx29 and Cx32 were examined in relation to the astrocytic connexins Cx30 and Cx43, and the previously reported detection of Cx32 densely distributed along myelinated fibers (Li et al., 1997) was reinvestigated by using wild type (WT) and Cx32 knockout (KO) mice.

MATERIALS AND METHODS

Antibodies, animals, and western blotting

The anti-connexin antibodies used in this study, in addition to sources and citations reporting their specificity characteristics, are listed in Table 1. The anti-Cx29 antibody has been

characterized with respect to specificity of Cx29 detection in sciatic nerve and in HeLa cells transfected with Cx29 cDNA (Li et al., 2002). This antibody was developed and supplied by Zymed Laboratories (South San Francisco, CA), and the peptide sequence within Cx29 against which the antibody was raised is proprietary. Polyclonal anti-Cx43 antibody 18A and monoclonal anti-Cx32 7C7 were generously provided by E. L. Hertzberg. For immunolabeling markers of oligodendrocytes and myelin, additional antibodies were monoclonal anti–2,′3′-cyclic nucleotide 3′-phosphodiesterase (CNPase; Sternberger Monoclonals, Baltimore, MD), polyclonal anti-CNPase (provided by Dr. P. E. Braun, McGill University, Montreal, QC, Canada), and monoclonal anti–myelin-associated glycoprotein (MAG; Chemicon International, Temecula, CA).

Seventy-two adult male CD1 mice (30 –40 g), including 25 at various developmental ages, and four adult male Sprague-Dawley rats (300 –350 g) were obtained from Central Animal Services at the University of Manitoba and treated according to approved protocols of the Central Animal Care Committee. In addition, Cx32 KO C57BL/6 mice were provided by K. Willecke (Bonn, Germany) and, with WT C57BL/6 mice, were bred at Colorado State University according to standard protocols. Eight WT and nine KO animals were used.

For biochemical analyses, adult mice were decapitated, the brains and spinal cords were removed, and various brain regions were dissected out and stored at −80°C until use. Tissues were similarly dissected out from mice at postnatal ages 1, 7, 14, and 20 days. Whole brains pooled from six mice (repeated twice) were used for subcellular fractionation by discontinuous sucrose density gradient ultracentrifugation, as previously described (Li et al., 1997; Lynn et al., 2001). The material obtained included a combined synaptosomal and mitochondrial fraction (P2), microsomal/plasma membrane fraction (P3), a soluble fraction, a synaptosomal fraction, and a myelin fraction. Western blotting of Cx29 and Cx32 by sodium dodecylsulfate polyacrylamide gel electrophoresis was conducted as previously described (Li et al., 1997; 2002; Lynn et al., 2001). For regional analysis of Cx29 expression and comparisons of Cx29 levels in subcellular fractions, lanes were loaded with equal amounts of protein from homogenates of brain regions or subcellular fractions.

Light microscopic immunofluorescence

Mice were deeply anesthetized with equithesin (3 ml/kg; Scadding, 1981) and transcardially perfused with 3 ml of pre-fixative consisting of cold (4°C) 0.1 M sodium phosphate buffer (PB), pH 7.4, containing 0.9% saline, 0.1% sodium nitrite, and heparin (1 U/ml). This was followed by perfusion with 20, 40, or 60 ml of cold 0.16 M sodium PB, pH 7.6, containing 4% formaldehyde and 0.2% picric acid. For protocols involving postfixation, brains were removed, sectioned into transverse blocks 2 mm thick, placed into perfusion fixative for 1.5 hours, and then stored at 4°C in cryoprotectant (50 mM PB, 10% sucrose, and 0.2% sodium azide) for a minimum of 48 hours before sectioning. For protocols avoiding postfixation, fixative was flushed from animals by perfusion with 10 ml of PB, pH 7.4, containing 10% sucrose. Brains were removed, blocked, and stored in cryoprotectant, as described above. For developmental studies, mouse pups at postnatal days 8, 14, and 20 were perfused as above except with solution volumes adjusted for body weight. Brains from 2-day-old mice were immersion fixed for 2 to 4 hours in cold 0.16 M sodium PB, pH 7.6, containing 4% formaldehyde and 0.2% picric acid. Optimal immunohistochemical labeling for Cx29 was achieved by perfusion with 40 to 60 ml of fixative, with little discernible difference in labeling with or without postfixation. Optimal immunolabeling for Cx32 was obtained by perfusion with 20 to 40 ml of fixative without postfixation. Immunolabeling for Cx30 and Cx43 was equally robust with all the fixation protocols.

Ten-micron transverse sections were cut on a cryostat, collected on gelatinized glass slides, and stored at −34°C. After storage, sections on slides were washed extensively in 50 mM of

Tris-HCl, pH 7.4, containing 1.5% sodium chloride (TBS) and 0.3% Triton X-100 (TBST). All sections were incubated with primary and secondary antibodies diluted in TBST containing 4% normal goat serum. Anti-connexin antibodies were used at the dilutions reported in Table 1. Monoclonal anti-CNPase was diluted to 1:5,000, polyclonal CNPase was diluted to 1:500, and anti-MAG was diluted to 1:500. Sections processed for double immunofluorescence labeling were simultaneously incubated with two different primary antibodies for 24 hours at 4°C. Sections were then washed for 1 hour in TBST and incubated simultaneously with two appropriate secondary antibodies for 1.5 hours at room temperature. A similar protocol was used for triple immunofluorescence labeling. Secondary antibodies were fluorescein isothiocyanate–conjugated horse anti-mouse immunoglobulin G (IgG; Vector Laboratories, Burlingame, CA.) diluted to 1:100, Cy3-conjugated donkey anti-rabbit IgG (Jackson ImmunoResearch Labs, West Groove, PA) diluted to 1:200, Cy3-conjugated goat anti-mouse IgG (Jackson ImmunoResearch Labs) diluted to 1:200, AlexaFluor488 $F(ab')_2$-conjugated goat anti-rabbit (Molecular Probes, Eugene, OR) diluted to 1:1,000, Cy5-conjugated donkey anti-mouse IgG (Jackson Immunoresearch Labs) diluted to 1:200, and Cy3-conjugated donkey anti-goat IgG (Jackson ImmunoResearch Labs) diluted to 1:200. After incubation with secondary antibodies, sections were washed for 20 minutes in TBST, followed by two 20-minute washes in TBS, and then coverslipped with anti-fade medium. In control procedures, omission of one or the other of the two primary antibodies with inclusion of both secondary antibodies produced no inappropriate labeling (i.e., secondary anti-rabbit recognition of mouse monoclonal primary or secondary anti-mouse recognition of rabbit polyclonal primary), indicating lack of cross reactions between antibodies.

Images were acquired on a Zeiss Axioskop2 fluorescence microscope and Olympus Fluoview IX70 confocal microscope with krypton/argon laser. For confocal analysis, double-labeled sections were scanned twice by using single laser excitation of a selected area for one fluorochrome and then single excitation of the same area for the other fluorochrome. Triple labeling was also conducted by single scans of selected areas for each fluorochrome. Precisely the same area for each fluorochrome was scanned to obtain images of double or triple labeling, and images were not manipulated to alter alignment of resulting overlays. Digital images were acquired with a 60× oil-immersion objective lens (numerical aperture, 1.4) with sufficient confocal "zoom" magnification to discern individual immunolabeled puncta. Images at 1,024 × 1,024 pixel resolution were captured by using AxioVision 3.0.6 software and assembled in Photoshop 6.0 or Corel Draw 8. Minimal adjustment to brightness and contrast was required.

RESULTS

Cx29 expression in adult brain

Regional Cx29 expression in adult mouse CNS analyzed by western blotting is shown in Figure 1A. In all areas examined, Cx29 was detected as a monomer form at 31 to 33 kDa and as a presumptive dimer at 51 kDa. A protein of unknown identity was detected at 38 to 39 kDa in some brain regions but may have represented a breakdown product of dimeric Cx29. Although not quantified, Cx29 levels were highest in caudal CNS structures, including the brainstem, cerebellum, and spinal cord, moderate in thalamus and hypothalamus, and lowest in the cerebral cortex and hippocampus, indicating greater Cx29 expression in progressively more caudal CNS areas. Subcellular localization of Cx29, determined by western blotting of brain subcellular fractions, indicated that the myelin fraction contained the greatest abundance of Cx29 (Fig. 1B). Levels were low in the mixed mitochondrial/synaptosomal fraction (P2), barely detectable in the microsomal (P3) and pure synaptosomal fractions, and undetectable in the soluble fraction, where anti-Cx29 recognized instead a protein of unknown identity migrating slightly faster than the Cx29 dimer. Designation of the 51-kDa immunoreactive protein as dimeric

Cx29 was supported by the enrichment of this band in the myelin fraction being comparable to that of Cx29 monomer.

In view of anatomical results indicating Cx29 expression by oligodendrocytes (see below) and the documented expression of Cx32 by these cells, the detection and immunoblotting profile of Cx29 were compared with those of Cx32 in brain tissue from WT and Cx32 KO animals (Fig. 1C). In subcellular fractions of myelin, Cx29 and Cx32 appeared as distinctly different bands, with Cx29 migrating slightly more slowly than Cx32, indicating that anti-Cx29 does not cross react with Cx32 and, conversely, that anti-Cx32 does not cross react with Cx29. In homogenates of thalamus probed with anti-Cx32 antibody 7C7, Cx32 was detected in tissue from WT mice and was absent in Cx32 KO mice, thus confirming Cx32 recognition by this antibody. Similar results were obtained with the other antibodies listed in Table 1. In homogenates of thalamus probed with anti-Cx29 antibody, Cx29 was detected in WT and Cx32 KO mice, further indicating that the immunoreactive band designated Cx29 does not represent a cross reaction with Cx32. Comparable levels of Cx29 were observed in WT and Cx32 KO tissue, suggesting that deletion of the Cx32 gene had little effect on Cx29 expression. Detection of the epitope against which the anti-Cx29 antibody was raised is shown by western blotting in Figure 1D, with and without antibody preadsorption with peptide immunogen. Antibody preadsorption eliminated the monomer and dimer immunoreactive bands in homogenates of thalamus and the myelin subcellular fraction.

Cx29 localization in adult brain

Immunohistochemical labeling for Cx29 in various areas of the CNS is shown in Figure 2. In most regions of mouse CNS, intense Cx29 immunoreactivity was localized to fibers and fiber tracts. As shown in sections of olfactory bulb (Fig. 2A,B) and cerebral cortex (Fig. 2C,D), double immunofluorescence for the myelin and oligodendrocyte marker CNPase combined with Cx29 showed nearly identical patterns of fiber labeling. Localization of Cx29 along fibers often matched that of CNPase (Fig. 2E,F), suggesting an association of Cx29 with myelin. Although only evident at higher magnification, CNPase-immunopositive oligodendrocyte cell bodies displayed faint Cx29 immunofluorescence (Fig. 2E,F). No evidence was found for Cx29 labeling associated with neuronal or astrocyte cell bodies in any brain region examined, nor was labeling associated with leptomeningeal, vascular, or ependymal structures. Immunofluorescence for Cx29 was most intense in white and gray matter of the thalamus (Fig. 2G), globus pallidus (Fig. 2I), spinal cord (Fig. 2J), and brainstem (not shown), all of which contain dense concentrations of myelinated fibers. Regions with a paucity of labeling for CNPase, such as the striatum (Fig. 2I) and superficial layers (lamina II) of the spinal cord dorsal horn (Fig. 2J; CNPase not shown), also displayed sparse labeling for Cx29. All labeling was eliminated after preadsorption of anti-Cx29 antibody with cognate peptide, as illustrated in the thalamus (Fig. 2H). Comparisons of Cx29 immunoreactivity in mouse and rat CNSs, shown in sections through the dentate gyrus of the hippocampus, indicated that Cx29 labeling along fibers in mouse brain (Fig. 2K) was also evident in rat brain (Fig. 2L).

An exception to Cx29 association with CNPase-positive fibers and oligodendrocyte somata occurred in the cerebellum. Although CNPase/Cx29 colocalization was observed in cerebellar white matter and the granule cell layer, the molecular layer was devoid of labeling for CNPase (Fig. 2M) but displayed dense, punctate labeling with the anti-Cx29 antibody (Fig. 2N). The association of this labeling with astrocytes, Bergmann glial cells, or neurons in the cerebellar molecular layer remains to be determined. In western blots of the cerebellum compared with other brain regions, the anti-Cx29 antibody did not detect any additional bands that would suggest cross reaction with a cerebellar protein not present elsewhere in brain. However, we cannot exclude the possibility of such a cross reaction.

Cx29 in developing brain

The developmental profile of Cx29 expression was examined by western blotting of tissue homogenates from the cerebral cortex, thalamus, and brainstem at different postnatal ages. Blots are shown at optimal exposure time to film (Fig. 3, left column) and after film overexposure (Fig. 3, right column) to adequately illustrate the comparatively wide range of expression levels in different regions and at different ages. Cx29 was barely detectable at postnatal day 7 in all regions examined, even at long film exposure. At postnatal day 14, Cx29 levels were moderate in brainstem and undetectable in the thalamus and cerebral cortex at normal film exposure, but faintly present in the latter two regions after long exposure. From day 20 to adulthood, levels increased in each area, with an overall caudal-to-rostral pattern in onset time and relative abundance of Cx29.

Examination of Cx29 in combination with CNPase in mice at different ages indicated the first appearance of Cx29 at about postnatal day 8 in the corpus callosum, which contained some labeled fibers and oligodendrocytes (Fig. 4A,B). No labeling was evident elsewhere in the brain. By postnatal day 14, numerous Cx29-positive oligodendrocytes were observed in most brain areas, as shown by CNPase/Cx29 double labeling in the cerebral cortex (Fig. 4C,D). Many oligodendrocyte somata at this age were much more intensely labeled for Cx29 than in the adult brain, and each soma appeared to be associated with a surrounding field of weakly labeled fibers (Fig. 4D). Similar results were obtained at postnatal day 20, except that fewer oligodendrocyte cell bodies were intensely labeled, and labeling associated with myelinated fibers was increased. In the adult brain, a few oligodendrocyte somata per section displayed intense labeling (not shown) comparable to that seen during the second postnatal week. Faint, presumably nonspecific labeling of neuronal nuclei occurred in some preparations of CNS tissues from younger animals (Fig. 4D,F). Although most oligodendrocyte somata were intensely labeled for CNPase at postnatal days 14 and 20, a small proportion exhibited weak labeling at the later age, as shown in the hypothalamus (Fig. 4E). It appeared that weak labeling for CNPase was accompanied by intense labeling for Cx29 (Fig. 4F) and, conversely, diminished labeling for Cx29 was accompanied by the typically intense labeling for CNPase seen in the adult brain.

Confocal imaging of double labeling for CNPase and Cx29 at postnatal day 14 clearly demonstrated intense intracellular labeling for Cx29 within oligodendrocyte cell bodies and in their processes surrounding individual cells (Fig. 4G). At this age, Cx29 immunofluorescence occasionally could be followed continuously from cell bodies to several initial processes and along fibers forming Cx29-positive arbors around oligodendrocytes (Fig. 4H).

Cx29 colocalization with CNPase and MAG

Confocal immunofluorescence was used to examine co-localization of Cx29 with the oligodendrocyte markers CNPase and MAG. Anti-CNPase and anti-MAG antibodies produced robust labeling of fibers and oligodendrocyte somata throughout the CNS. CNPase was diffusely localized to cells, whereas MAG was granular (Fig. 5). In double-labeled sections, Cx29 along fibers and in oligodendrocyte somata was colocalized with CNPase, as shown in the thalamus (Fig. 5A) and the cerebral cortex (Fig. 5B), and with MAG, as shown in the cerebral cortex (Fig. 5C–E). By single scan imaging, Cx29 was distributed around the periphery of oligodendrocyte cell bodies, where it appeared as continuous labeling or as fine puncta associated with the plasma membrane (Fig. 5A2,B2,E2). Labeling for Cx29 was also observed intracellularly, where it had a granular appearance (Fig. 5E2), and displayed partial association with granules labeled for MAG (Fig. 5E). Cx29 exhibited greater colocalization with MAG along fibers (Fig. 5D).

Cx29 colocalization with Cx32

Confocal double immunofluorescence labeling for Cx32 and Cx29 was used to determine the extent of colocalization between Cx29 and Cx32. Both connexins were present on large- and small-diameter fibers. Labeling for Cx29 along fibers showed considerable, but not total, overlap with labeling for Cx32 (Fig. 6A). Large-diameter fibers were often more heavily labeled for Cx32 than for Cx29, despite the surrounding presence of smaller-diameter fibers that were intensely labeled for Cx29, suggesting that the occurrence of differential labeling was not an artifact of tissue fixation conditions. Immunofluorescence for Cx32 was seen as relatively large puncta decorating oligodendrocyte somata and extending for short distances along their initial processes (Fig. 6B1). Very little Cx32 was discernible intracellularly in these somata. This was in contrast to the much smaller Cx29 puncta associated with these cells, the virtual absence of Cx29 along their initial processes, and the abundance of Cx29 intracellularly (Fig. 6B2). Overlays of double labeling indicated that fine Cx29 puncta around the periphery of oligodendrocytes were frequently colocalized with the larger Cx32 puncta (Fig. 6B3). The distribution of Cx32 and Cx29 along individual fibers exhibited various patterns but was often punctate (Fig. 6C,E) or intermittent, spanning the width of fibers (Fig. 6D). Cx32 and Cx29 were partly colocalized at these sites. Colocalization along medium-size and small fibers was also evident but more variable, with one or the other connexin predominating. Confocal analysis of triple immunofluorescence labeling for Cx29, Cx32, and CNPase in brain sections was conducted to confirm that cells exhibiting coexpression of Cx32 (Fig. 6F1) and Cx29 (Fig. 6F2) were oligodendrocytes as demonstrated by their labeling for CNPase (Fig. 6F3) and overlap of labeling in merged images (Fig. 6F4).

Cx29 and Cx32 in relation to astrocytic connexins

Confocal analysis of astrocytic Cx43 and Cx30 in relation to Cx32 and Cx29 at gap junctions formed by oligodendrocytes is shown in Figure 7. Immunofluorescence for Cx43 throughout the brain appeared as densely distributed puncta, most of which represented labeling of gap junctions between astrocytes (Yamamoto et al., 1990a,b). However, a small percentage of these puncta was co-associated with punctate labeling for Cx32 on oligodendrocyte cell bodies and their processes, as shown in the hypothalamus (Fig. 7A) and the thalamus (Fig. 7B). These sites of co-association correspond to gap junctions between astrocytic Cx43 and oligodendrocytic Cx32, as previously reported (Rash et al., 2001). Confocal immunofluorescence of astrocytic Cx30 and oligodendrocytic Cx32 showed similar co-association of punctate labeling for these two connexins on oligodendrocyte cell bodies (Fig. 7C), consistent with the ultrastructural colocalization of Cx30 and Cx43 at astrocyte gap junctions with oligodendrocytes (Rash et al., 2001). Labeling of cells for CNPase and Cx30 confirmed that Cx30-positive puncta decorated the surface of oligodendrocytes (Fig. 7D). In contrast, confocal analysis of double labeling for Cx43 and Cx29 in numerous brain areas examined, and illustrated in the globus pallidus (Fig. 7E) and hypothalamus (Fig. 7F), showed only minor co-association of the two connexins at sites along the periphery of oligodendrocyte somata.

Confocal double labeling was undertaken to determine the degree to which Cx32 along myelinated fibers was associated with Cx43 and Cx30 in astrocytic processes that form gap junctions at abutments with myelinated fibers. As shown in the cerebral cortex (Fig. 7G) and thalamus (Fig. 7H), fields with relatively dense Cx43-positive puncta and robust labeling for Cx32 along myelinated fibers showed only occasional overlap of labeling for the two connexins along fibers. Similarly, in areas with dense labeling for Cx30, such as the thalamus (Fig. 7I) and habenula (Fig. 7J), labeling for Cx32 along myelinated fibers displayed only minor overlap with Cx30-immunopositive puncta. Thus, unlike Cx32 associated with oligodendrocyte somata, the bulk of Cx32 in oligodendrocyte processes that form myelin appeared to have little association with astrocytic elements.

Cx32 localization to myelinated fibers in brain was confirmed by using comparisons of Cx32 immunolabeling in WT and Cx32 KO mice. Anti-Cx32 antibody that showed an absence of Cx32 detection in brain of Cx32 KO mice by western blotting (Fig. 1C) produced robust labeling of CNPase-positive myelinated fibers throughout the brain of WT mice, as illustrated in the cerebral cortex (Fig. 8A). Authenticity of Cx32 labeling was indicated by the total absence of Cx32 immunoreactivity in a field of cerebral cortex containing dense labeling for CNPase in tissue from a Cx32 KO mouse (Fig. 8B). High magnification confocal micrographs of CNPase and Cx32 colocalization along myelinated fibers is shown in Figure 8C.

DISCUSSION

We found that Cx29 is expressed by oligodendrocytes throughout the CNS and that it is localized to these cells and their myelinating processes in adult and developing brains. These results were corroborated by documenting Cx29 enrichment in subcellular fractions of myelin as opposed to low levels in synaptosomal subfractions, which previously were reported to be enriched in astrocytic and neuronal connexins (Lynn et al., 2001). A similar localization of Cx32, including its presence in oligodendrocyte somata, dense concentration along myelinated fibers, and enrichment in myelin, as previously reported (Li et al., 1997), was supported by the current demonstration of a total absence of immunofluorescence labeling and western blot detection of Cx32 in Cx32 KO mice. Despite their cellular coexpression, Cx29 was minimally colocalized with Cx32 on oligodendrocyte somata and only partly co-localized with Cx32 along myelinated fibers. The only departure from Cx29 localization exclusively in oligodendrocytes occurred in the molecular layer of the cerebellum, which was devoid of labeling for CNPase but contained dense immunoreactivity with anti-Cx29 antibody. The identity of the protein detected in this cerebellar subregion and its subcellular localization remain to be determined.

In the peripheral nervous system (PNS), Cx29 localization described recently by Altevogt et al. (2002) is in agreement with our light microscopic and freeze-fracture replica immunogold labeling observations of Cx29 in the sciatic nerve (Li et al., 2002). In the CNS, however, Altevogt et al. (2002) reported Cx29 and Cx32 expression in mutually exclusive subsets of oligodendrocytes in spinal cord and noted similar expression patterns in the olfactory bulb, cerebrum, cerebellum, and pons. In contrast, after examination of more than 50 oligodendrocytes per section encompassing many CNS regions, including the spinal cord, in more than 100 sections taken from more than 20 brains, we found that virtually all CNPase-positive oligodendrocyte somata contained Cx29 and Cx32. Altevogt et al. (2002) also reported Cx29 and Cx32 localization to mutually exclusive subsets of myelin sheaths in the CNS, whereas our findings indicated partial colocalization of these connexins along many fibers. Reasons for these disparities may be due to differences in tissue preparation and differences in efficiency of connexin detection by different antibodies.

Connexins at astrocyte/oligodendrocyte junctions

It is becoming clear that gap junctions linking cells in the panglial syncytium are composed of multiple connexins with selective cellular expression patterns: Cx26, Cx30, and Cx43 in astrocytes and Cx32, Cx29 and Cx47 in oligodendrocytes (Nagy et al., 1997, 1999, 2001, 2003a,Nagy et al., b; Rash and Yasumura, 1999; Rash et al., 1997, 2001; Altevogt et al., 2002). The presence of six different connexins in macroglial cells raises questions concerning the extent to which GJIC within the syncytium is regulated by the organization of connexin coupling partners at A/O gap junctions. In particular, the non-permissiveness of Cx43 coupling with Cx32 (White and Bruzzone 1996) in addition to the present findings that Cx29 is very sparsely distributed on oligodendrocyte somata in adult brain and exhibits only minor colocalization with Cx43 on these somata suggest little, if any, Cx32/Cx43 or Cx29/Cx43

coupling at A/O junctions. Further, it can be more generally inferred that Cx29 is minimally co-associated with astrocytic Cx26 and Cx30 at A/O gap junctions in the adult brain. Oligodendrocytes have been reported to express Cx45 (Dermietzel et al., 1997; Kunzelmann et al., 1997) and Cx43/45 coupling is permissive for functional channel formation (Bruzzone et al., 1996; White and Bruzzone, 1996). However, widespread expression of Cx45 in oligodendrocytes has not been documented. Astrocytic Cx43 at A/O junctions more likely couples with Cx47, which is strongly expressed in oligodendrocytes and exhibits immunolabeling patterns similar to that of Cx32 on oligodendrocyte somata (Nagy et al., 2003a). This idea was supported in a recent study involving Cx32 KO mice, in which astrocytic Cx26 and Cx30 were reduced and astrocytic Cx43 and oligodendrocytic Cx47 remained densely concentrated on oligodendrocyte somata despite the absence of Cx32 (Nagy et al., 2003b).

Cx29 expression during CNS development

Examination of Cx29 levels during development indicated a temporal and spatial expression pattern consistent with the known onset time and caudal-to-rostral progression of myelination along the neuraxis (Verity and Campagnoni, 1988). Unlike transiently elevated levels of several connexins during brain development (Prime et al., 2000), Cx29 protein continuously increased to maximum levels in the adult CNS. The shift from robust immunolabeling for Cx29 in oligodendrocyte cell bodies at young ages to much lower levels in mature somata and increasing levels along myelinated fibers indicate a primary function of Cx29 in mature myelin. Distinct patterns of labeling for Cx29 and Cx32 around oligodendrocytic somata and their differential detection intracellularly may reflect segregation of connexin trafficking in these cells. In studies of other cell types expressing two different connexins, it appears that intracellular trafficking routes from the endoplasmic reticulum to gap junctional plaques can occur via different pathways involving a Golgi-microtubule transport system or a Golgi-independent process (George et al., 1999, Jordan et al., 1999, Martin et al. 2001; Lauf et al., 2002; Gaietta et al., 2002). Thus, Cx29 and Cx32 in oligodendrocytes may contain different subcellular targeting signals, as has been reported for other connexins (Martin et al., 2001), and may be packaged and transported differently. This notion is supported by our previous ultrastructural observations of an association of oligodendrocytic Cx32 with endoplasmic reticulum with no evidence of its intracellular vesicular localization (Li et al., 1997) and preliminary observations of an association of Cx29 with vesicular elements in these cells (A. Sik, unpublished observations). The lack of Cx29 detection in the initial processes of oligodendrocytes in the adult brain, despite its presence in myelin, suggests the involvement of trafficking pathway resulting in transient epitope masking during exit of Cx29 from somal to fiber compartments. Alternatively, transit through initial processes may be very rapid, and low levels at these sites may preclude detection.

Connexins in myelin

One possible function for connexins in CNS myelin is gap junction formation between non-compacted cytoplasmic compartments at the outer loop of myelin and astrocytic elements that abut these internodal myelin compartments. The occurrence, if not the frequency, of such A/O gap junctions has been well documented (Luizzi and Miller, 1987; Massa and Mugnaini, 1982; Waxman and Black, 1984) and includes demonstrations of Cx43 on the astrocytic side of such junctions (Ochalski et al., 1997; Rash et al., 2001). Our results showing a paucity of an association Cx43 with Cx32 along myelinated fibers suggests that A/O junctions along these fibers is unlikely to account for the abundance of oligodendrocytic connexins in myelin. An additional and/or alternative possibility involves Cx29 and Cx32 localization at paranodal loops and Schmidt-Lanterman incisures, as seen in peripheral nerves (Li et al., 2002; Altevogt et al., 2002). Incisures have been observed in vivo in nerves of living animals (Williams and Hall, 1970), and electron microscopic studies of PNS have shown that they consist of short,

circumferential dilations of Schwann cell cytoplasm spanning the full breath of myelin along internodal regions (Hall and Williams, 1970; Friede and Samorajski, 1969; Ghabriel and Allt, 1981). Considering that myelin lamellae surrounding axons form impermeable barriers to diffusion of substances, Schmidt-Lanterman incisures may provide a route for metabolic support and maintenance of myelin sheaths (Webster, 1965; Williams and Hall, 1971a,b; Ghabriel and Allt, 1981). It has also been proposed that connexins at incisures form autologous or reflexive gap junctions between successive inner to outer cytoplasmic membranes, thereby providing a pathway consisting of a series of gap junction channels for radial diffusion of ions and metabolites (Bergoffen et al., 1993; Scherer et al., 1995; Scherer, 1996; Bone et al., 1997; Balice-Gordon et al., 1998; Arroyo and Scherer, 2000).

The existence of Schmidt-Lanterman incisures within CNS myelin has been firmly established However, unlike the conical arrangement of successive radial cytoplasmic pockets at incisures in peripheral nerves, incisures in the CNS occur as series of pockets coursing radially in a zig-zag manner, do not always extend from the outermost to the innermost myelin lamella, and apparently are present only in the largest of central myelinated fibers (Bunge et al., 1960; Hirano and Dembitzer, 1967; Conradi, 1969; Hildebrand, 1971; Blakemore, 1969; Hildebrand et al., 1993). If Cx29 and Cx32 are concentrated at incisures in the CNS, then differences in the central and peripheral organizations of these structures may account for differences in connexin labeling patterns observed in CNS as opposed to PNS myelin. Moreover, our observations of the presence of Cx32 and Cx29 along a large proportion of CNPase-positive fibers might have been interpreted as suggesting a wider occurrence of Schmidt-Lanterman incisures in the CNS than previously believed.

A more likely alternative is that Schmidt-Lanterman incisures may indeed be rare in the CNS, as reported, and that Cx29 and/or Cx32 may be only partly localized to these structures in central myelin, as suggested by our observations. First, although many fibers contained Cx29 and Cx32, some had a preponderance of one or the other connexin. Because all oligodendrocytes express both connexins, differential labeling of fibers for Cx29 and Cx32 was unlikely to be due to mutually exclusive expression of these connexins by subpopulations of oligodendrocytes, but rather to differential transport from somata to myelin. Second, the partial colocalization of Cx29 and Cx32 along individual fibers suggests some degree of functional independence of these proteins in myelin. Third, although MAG is highly concentrated at incisures in the PNS, it does not appear to be enriched at these structures in the CNS (Trapp et al., 1989), yet it exhibited colocalization with Cx29 and Cx32 in central myelin. Together these points suggest targeting of one or both of these connexins to several subcellular compartments in CNS myelin, thus excluding their restricted localization to Schmidt-Lanterman incisures. The localization of connexins in CNS myelin sheaths remains to be determined by electron microscopic methods, in particular whether gap junctions are present at incisures, whether Cx29 and Cx32 contribute to the formation of such junctions, and whether these connexins have additional as yet undetermined functions, as previously discussed (Li at al., 2002).

Acknowledgements

We thank B. McLean and N. Nolette for excellent technical assistance. We also thank Dr. P. E. Braun for the generous gift of polyclonal anti-CNPase, Dr. E. L. Hertzberg for providing monoclonal anti-Cx32 antibody 7C7 and polyclonal antibody 18A, and Dr. K. Willecke for supplying Cx32 KO mice.

References

Altevogt BM, Kleopa KA, Postma FR, Scherer SS, Paul DL. Connexin29 is uniquely distributed within myelinating glial cells of the central and peripheral nervous systems. J Neurosci 2002;22:6458–6470. [PubMed: 12151525]

Arroyo EJ, Scherer SS. On the molecular architecture of myelinated fibres. Histochem Cell Biol 2000;113:1–18. [PubMed: 10664064]

Balice-Gordon RJ, Bone LJ, Scherer SS. Functional gap junctions in the Schwann cell myelin sheath. J Cell Biol 1998;142:1095–1104. [PubMed: 9722620]

Bergoffen J, Scherer SS, Wang S, Oronzi-Scott M, Bone L, Paul DL, Chen K, Lensch MW, Chance P, Fischbeck K. Connexin mutations in X-linked Charcot-Marie-Tooth disease. Science 1993;262:2039 –2042. [PubMed: 8266101]

Bone LJ, Deschênes SM, Balice-Gordon RJ, Fischbeck KH, Scherer SS. Connexin 32 and X-linked Charcot-Marie-Tooth disease. Neurobiol Dis 1997;4:221–230. [PubMed: 9361298]

Blakemore WF. Schmidt-Lanterman incisures in the central nervous system. J Ultrastruct Res 1969;29:496 –498. [PubMed: 5365373]

Bruzzone R, White TW, Paul DL. Connections with connexins: the molecular basis of direct intercellular signaling. Eur J Biochem 1996;238:1–27. [PubMed: 8665925]

Bunge RP, Bunge MB, Ris R. Electron microscopic study of demyelination in an experimentally induced lesion in adult cat spinal cord. J Biophys Biochem Cytol 1960;7:685–696. [PubMed: 13805917]

Conradi S. Observations on the ultrastructure of the axon hillock and initial axon segment of lumbosacral motoneurons in the cat. Acta Physiol Scand Suppl 1969;332:65–84. [PubMed: 5386536]

Dahl E, Manthey D, Chen Y, Schwarz H-J, Chang S, Lalley PA, Nicholson BJ, Willecke K. Molecular cloning and functional expression of mouse connexin30, a gap junction gene highly expressed in adult brain and skin. J Biol Chem 1996;271:17903–17910. [PubMed: 8663509]

Dermietzel R, Traub O, Hwang TK, Beyer E, Bennett MVL, Spray DC, Willecke K. Differential expression of three gap junction proteins in developing and mature brain tissues. Proc Nat Acad Sci USA 1989;86:10148 –10152. [PubMed: 2557621]

Dermietzel R, Farooq M, Kessler JA, Hertzberg EL, Spray DC. Oligodendrocytes express gap junction proteins connexin32 and connexin45. Glia 1997;20:101–114. [PubMed: 9179595]

Friede R, Samorajski T. The clefts of Schmidt-Lanterman: a quantitative electron microscopic study of their structure in developing and adult sciatic nerves of the rat. Anat Rec 1969;165:89 –102. [PubMed: 5806361]

Gaietta G, Deerinck TJ, Adams SR, Bouwer J, Tour O, Laird DW, Sosinsky GE, Tsien RY, Ellisman MH. Multicolor and electron microscopic imaging of connexin trafficking. Science 2002;296:503–507. [PubMed: 11964472]

George CH, Kendall JM, Evans WH. Intracellular trafficking pathways in the assembly of connexins into gap junctions. J Biol Chem 1999;274:8678 –8685. [PubMed: 10085106]

Ghabriel MN, Allt G. Incisures of Schmidt-Lanterman. Prog Neurobiol 1981;17:25–58. [PubMed: 7323300]

Hall SM, Williams PL. Studies of the incisures of Schmidt and Lanterman. J Cell Sci 1970;6:767–791. [PubMed: 5452094]

Hildebrand C. Ultrastructural and light-microscopic studies of the nodal region in large myelinated fibers of the adult feline spinal cord white matter. Acta Physiol Scand Suppl 1971;364:43–79. [PubMed: 4109394]

Hildebrand C, Remahl S, Persson H, Bjartmar C. Myelinated nerve fibers in the CNS. Prog Neurobiol 1993;40:319 –384. [PubMed: 8441812]

Hirano A, Dembitzer HM. A structural analysis of the myelin sheath in the central nervous system. J Cell Biol 1967;34:555–567. [PubMed: 6035645]

Jordan K, Salan JL, Dominquez M, Sia M, Hand A, Lampe PD, Laird DW. Trafficking, assembly, and function of a connexin Cx43-green fluorescent protein chimera in live mammalian cells. Mol Biol Cell 1999;10:2033–2050. [PubMed: 10359613]

Kunzelmann P, Blumcke I, Traub O, Dermietzel R, Willecke K. Coexpression of connexin45 and -32 in oligodendrocytes of rat brain. J Neurocytol 1997;26:17–22. [PubMed: 9154525]

Kunzelmann P, Schröder W, Traub O, Steinhäuser C, Dermietzel R, Willecke K. Late onset and increasing expression of the gap junction protein connexin30 in adult murine brain and long-term cultured astrocytes. Glia 1999;25:111–119. [PubMed: 9890626]

Lauf U, Giepmans BNG, Lopez P, Braconnot S, Chen S-S, Falk MM. Dynamic trafficking and delivery of connexons to the plasma membrane and accretion to gap junctions in living cells. Proc Natl Acad Sci USA 2002;99:10446 –10451. [PubMed: 12149451]

Li J, Hertzberg EL, Nagy JI. Connexin32 in oligodendrocytes and association with myelinated fibers in mouse and rat brain. J Comp Neurol 1997;379:571–591. [PubMed: 9067844]

Li WEI, Ochalski PAY, Hertzberg EL, Nagy JI. Immunorecognition, ultrastructure and phosphorylation of astrocytic gap junctions and connexin43 in rat brain after cerebral focal ischemia. Eur J Neurosci 1998;10:2444 –2463. [PubMed: 9749772]

Li X, Lynn BD, Olson C, Meier C, Davidson KG, Yasumura T, Rash JE, Nagy JI. Connexin29 expression, immunocytochemistry and freeze-fracture replica immunogold labelling (FRIL) in sciatic nerve. Eur J Neurosci 2002;16:795–806. [PubMed: 12372015]

Luizzi FJ, Miller RH. Radially oriented astrocytes in the normal adult rat spinal cord. Brain Res 1987;403:385–388. [PubMed: 2435373]

Lynn BD, Rempel JL, Nagy JI. Enrichment of neuronal and glial connexins in the postsynaptic density subcellular fraction of rat brain. Brain Res 2001;898:1–8. [PubMed: 11292443]

Martin PE, Blundell G, Ahmad S, Errington RJ, Evans WH. Multiple pathways in the trafficking and assembly of connexin 26, 32 and 43 into gap junction intercelluar communication channels. J Cell Sci 2001;114:3845–3855. [PubMed: 11719551]

Massa PT, Mugnaini E. Cell junctions and intramembrane particles of astrocytes and oligodendrocytes: a freeze-fracture study. Neuroscience 1982;7:523–538. [PubMed: 7078735]

Mugnaini, E. Cell junctions of astrocytes, ependyma, and related cells in the mammalian central nervous system, with emphasis on the hypothesis of a generalized functional syncytium of supporting cells. In: Fedoroff, S.; Vernadakis, A., editors. Astrocytes. 1. New York: Academic Press; 1986. p. 329-371.

Nagy, JI.; Dermietzel, R. Gap junctions and connexins in the mammalian central nervous system. In: Hertzberg, EL., editor. Advances in molecular and cell biology. 30. Greenwich: JAI Press; 2000. p. 323-396.

Nagy JI, Rash JE. Connexins and gap junctions of astrocytes and oligodendrocytes in the CNS. Brain Res Rev 2000;32:29 –44. [PubMed: 10751655]

Nagy JI, Ochalski PAY, Li J, Hertzberg EL. Evidence for colocalization of another connexin with connexin43 at astrocytic gap junctions in rat brain. Neuroscience 1997;78:533–548. [PubMed: 9145808]

Nagy JI, Patel D, Ochalski PAY, Stelmack GL. Connexin30 in rodent, cat and human brain: Selective expression in gray matter astrocytes, co-localization with connexin43 at gap junctions and late developmental appearance. Neuroscience 1999;88:447–468. [PubMed: 10197766]

Nagy JI, Li X, Rempel J, Stelmack G, Patel D, Staines WA, Yasumura T, Rash JE. Connexin26 in adult rodent CNS: demonstration at astrocytic gap junctions and co-localization with connexin30 and connexin43. J Comp Neurol 2001;441:302–323. [PubMed: 11745652]

Nagy JI, Dudek FE, Rash JE. Update on connexins and gap junctions in neurons and glia in the mammalian nervous system. Brain Res Rev. 2003aIn press

Nagy JI, Ionescu AV, Lynn BD, Rash JE. Coupling of astrocyte connexins Cx26, Cx30, Cx43 to oligodendrocyte Cx29, Cx32, Cx47: Implications from normal and Cx32 knockout mice. Glia. 2003bIn press

Ochalski PAY, Frankenstein UN, Hertzberg EL, Nagy JI. Connexin43 in rat spinal cord: localization in astrocytes and identification of heterotypic astro-oligodendrocytic gap junctions. Neuroscience 1997;76:931–945. [PubMed: 9135062]

Prime G, Horn G, Sutor B. Time-related changes in connexin mRNA abundance in the rat neocortex during postnatal development. Dev Brain Res 2000;119:111–125. [PubMed: 10648878]

Rash JE, Yasumura T. Direct immunogold labeling of connexins and aquaporin4 in freeze-fracture replicas of liver, brain and spinal cord: factors limiting quantitative analysis. Cell Tissue Res 1999;296:307–321. [PubMed: 10382274]

Rash JE, Duffy HS, Dudek FE, Bilhartz BL, Whalen LR, Yasumura T. Grid-mapped freeze-fracture analysis of gap junctions in gray and white matter of adult rat central nervous system, with evidence for a “panglial syncytium” that is not coupled to neurons. J Comp Neurol 1997;388:265–292. [PubMed: 9368841]

Rash JE, Staines WA, Yasumura T, Patel D, Hudson CS, Stelmack GL, Nagy JI. Immunogold evidence that neuronal gap junctions in adult rat brain and spinal cord contain connexin36 but not Cx32 or Cx43. Proc Natl Acad Sci USA 2000;97:7573–7578. [PubMed: 10861019]

Rash JE, Yasumura T, Dudek FE, Nagy JI. Cell-specific expression of connexins and evidence of restricted gap junctional coupling between glial cells and between neurons. J Neurosci 2001;21:1983–2000. [PubMed: 11245683]

Scadding JW. Development of ongoing activity, mechanosensitivity, and adrenaline sensitivity in severed peripheral nerve axons. Exp Neurol 1981;73:345–364. [PubMed: 7262242]

Scherer SS. Molecular specializations at nodes and paranodes in peripheral nerve. Microsc Res Tech 1996;34:452–461. [PubMed: 8837021]

Scherer SS, Deschennes SM, Xu Y-T, Grinspan JP, Fischbeck KH, Paul DL. Connexin32 is a myelin-related protein in the PNS and CNS. J Neurosci 1995;15:8281–8294. [PubMed: 8613761]

Severs NJ. Cardiovascular disease. Novartis Found Symp 1999;219:188 –206. [PubMed: 10207905]

Sohl G, Eiberger J, Jung YT, Kozak CA, Willecke K. The mouse gap junction gene connexin29 is highly expressed in sciatic nerve and regulated during brain development. Biol Chem 2001;382:973–978. [PubMed: 11501764]

Trapp BD, Andrews SB, Cootauco C, Quarles R. The myelin-associated glycoprotein is enriched in multivesicular bodies and peri-axonal membranes of actively myelinating oligodendrocytes. J Cell Biol 1989;109:2417–2426. [PubMed: 2478568]

Veenstra RD. Size and selectivity of gap junction channels formed from different connexins. J Bioenerg Biomembr 1996;28:327–337. [PubMed: 8844330]

Verity AN, Campagnoni AT. Regional expression of myelin protein genes in the developing mouse brain: in situ hybridization studies. J Neurosci Res 1988;21:238 –248. [PubMed: 2464076]

Waxman SG, Black JA. Freeze-fracture ultrastructure of the peri-nodal astrocyte and associated glial junctions. Brain Res 1984;308:77–87. [PubMed: 6434150]

Webster HF. The relationship between Schmidt-Lanterman incisures and myelin segmentation during Wallerian degeneration. Ann NY Acad Sci 1965;122:29 –38. [PubMed: 14313489]

White TW, Bruzzone R. Multiple connexin proteins in single intercellular channels: connexin compatibility and functional consequences. J Bioenerg Biomembr 1996;28:339 –350. [PubMed: 8844331]

Williams PL, Hall SM. In vivo observations on mature myelinated nerve fibers of the mouse. J Anat 1970;107:31–38. [PubMed: 5473291]

Williams PL, Hall SM. Prolonged in vivo observations of normal peripheral nerve fibers and their acute reactions to crush and deliberate trauma. J Anat 1971a;108:397–408. [PubMed: 5575308]

Williams PL, Hall SM. Chronic Wallerian degeneration—an in vivo and ultrastructural study. J Anat 1971b;109:487–503. [PubMed: 4949291]

Wolburg H, Rohlmann A. Structure–function relationships in gap junctions. Int Rev Cytol 1995;157:315–373. [PubMed: 7706021]

Yamamoto T, Ochalski PAY, Hertzberg EL, Nagy JI. LM and EM immunolocalization of the gap junctions protein connexin43 in rat brain. Brain Res 1990a;508:313–319. [PubMed: 2155040]

Yamamoto T, Ochalski PAY, Hertzberg EL, Nagy JI. On the organization of astrocytic gap junctions in the brain as suggested by LM and EM immunocytochemistry of connexin43 expression. J Comp Neurol 1990b;302:853–883. [PubMed: 1964467]

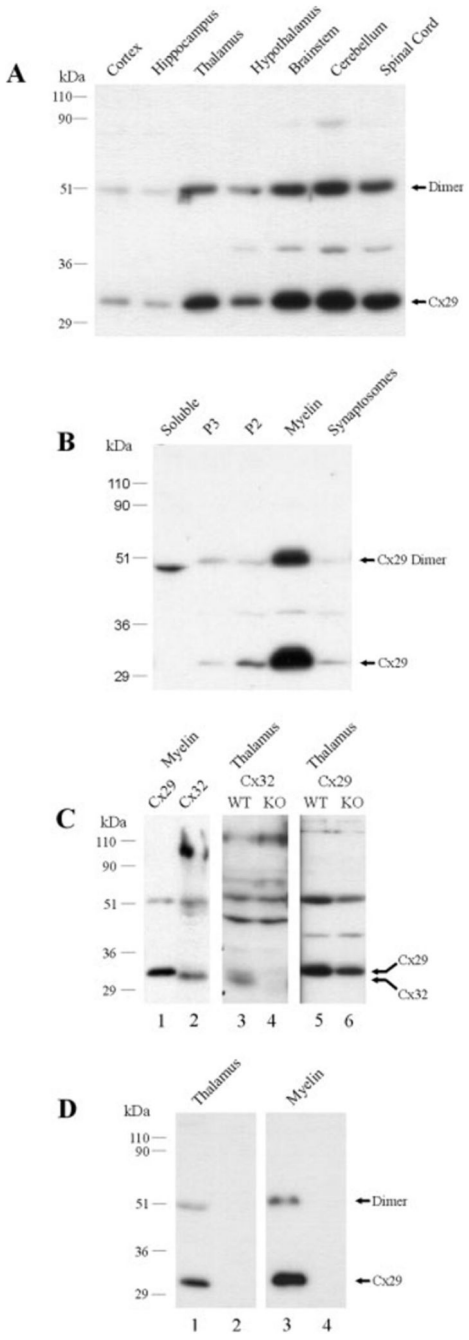

Fig. 1.

Western blots of Cx29 and Cx32 in various neural tissues. In all blots, numbers at left correspond to molecular weight markers. **A:** Immunoblot showing regional levels of Cx29 in adult mouse brain. Monomeric and presumptive dimeric Cx29 are detected at 31 to 33 kDa and at 51 kDa, respectively. **B:** Immunoblot showing Cx29 in soluble, microsomal membrane (P3), mitochondrial/synaptosomal (P2), myelin, and synaptosomal subcellular fractions of adult brain. Cx29 is concentrated in the myelin fraction, and a protein of unknown identity at 48 kDa is detected in the soluble fraction. **C:** Immunoblots comparing Cx29 and Cx32 migration profiles. Lanes loaded with protein from myelin fraction and from thalamus homogenate of WT and Cx32 KO mice were probed with the antibodies indicated. Cx29 and

Cx32 appear as distinct bands, and Cx32 at 30 to 31 kDa in the WT thalamus is absent in the Cx32 KO thalamus. Anti-Cx29 antibody detects Cx29 as corresponding bands in WT and Cx32 KO thalami. **D:** Immunoblots of the tissues indicated show elimination of Cx29 detection (lanes 2 and 4) after preadsorption of anti-Cx29 antibody with cognate peptide. Cx, connexin; KO, knockout; WT, wild type.

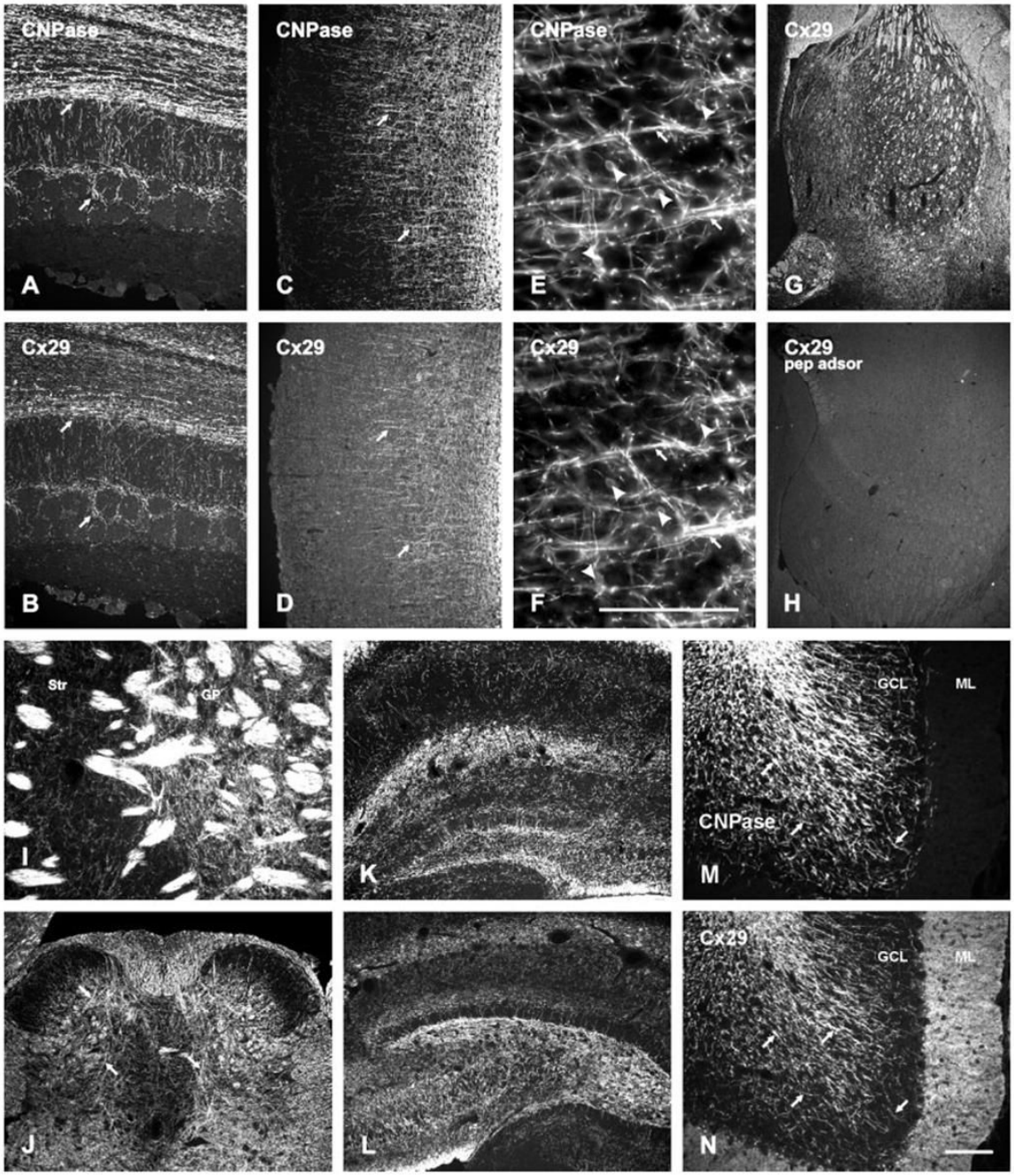

Fig. 2.

Immunofluorescence micrographs showing Cx29 localization in the CNS. **A–D:** Fields in olfactory bulb (A,B) and cerebral cortex (C,D) show overlapping distributions of fibers double labeled for CNPase (A,C, arrows) and Cx29 (B,D, arrows). **E,F:** Magnification of cerebral cortex showing colocalization of CNPase (E) and Cx29 (F) along myelinated fibers (arrows) and oligodendrocyte somata (arrowheads). **G,H:** Area in the thalamus (dorsal to the left) showing labeling for Cx29 (G) and elimination of labeling after preadsorption of anti-Cx29 with cognate peptide (H). **I:** Field at the border between the striatum (Str) and globus pallidus (GP) showing Cx29 in fiber bundles and in fibers scattered in neuropil of the GP. **J:** Lumbar spinal cord showing Cx29 in white matter and in myelinated fibers coursing through gray

matter (arrows). **K,L:** Dentate gyrus of the hippocampus comparing labeling for Cx29 in sections from mouse (K) and rat (L) brains. **M,N:** Field in a cerebellar folia showing colocalization of CNPase (M) and Cx29 (N) along myelinated fibers (arrows) in white matter and in the granule cell layer (GCL). Dense immunoreactivity with anti-Cx29 is also seen in the molecular layer (ML), which is devoid of CNPase-positive fibers. CNPase, 2,′3′-cyclic nucleotide 3′-phosphodiesterase; Cx, connexin. Scale bars = 100 μm for E, F in and for A–D and G–N in N.

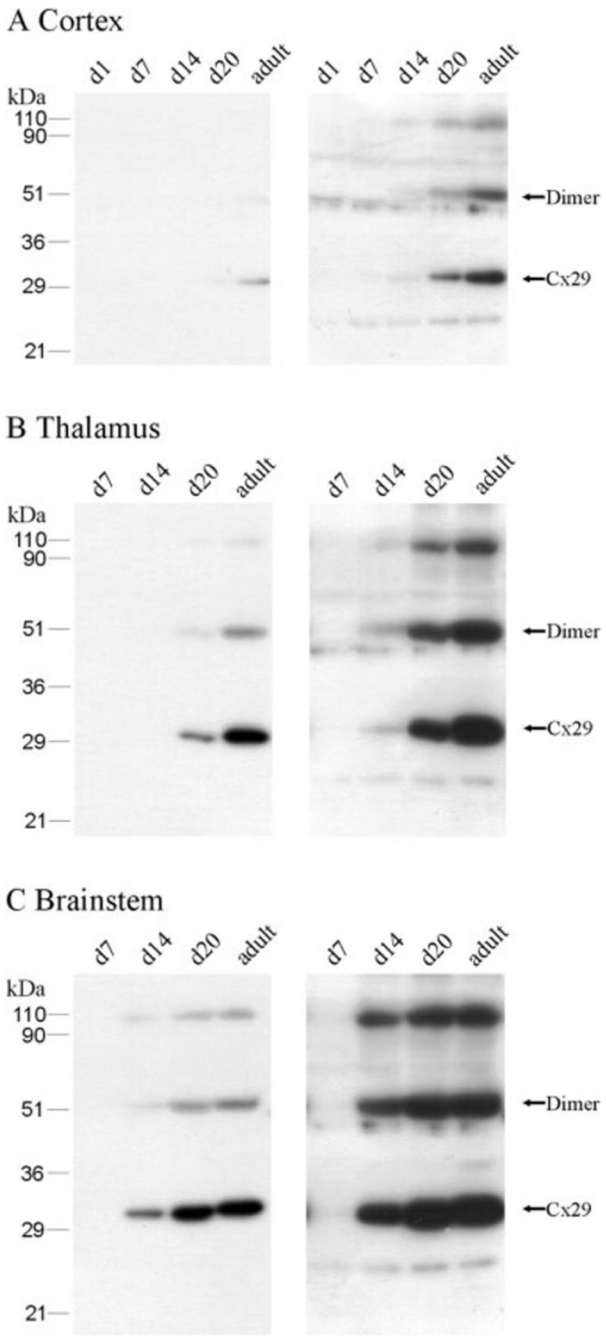

Fig. 3.

Western blots showing Cx29 levels in the cerebral cortex (**A**), thalamus (**B**), and brainstem (**C**) during development. Lanes were loaded with equal amounts of protein from homogenates of structures at the postnatal ages in days (d) indicated. For comparison of levels, blots are shown after exposure to film for short (left blot for each structure) and long (right blot for each structure) durations. Cx29 levels are highest in the adult brain, with increasing expression in each area during development. Cx, connexin.

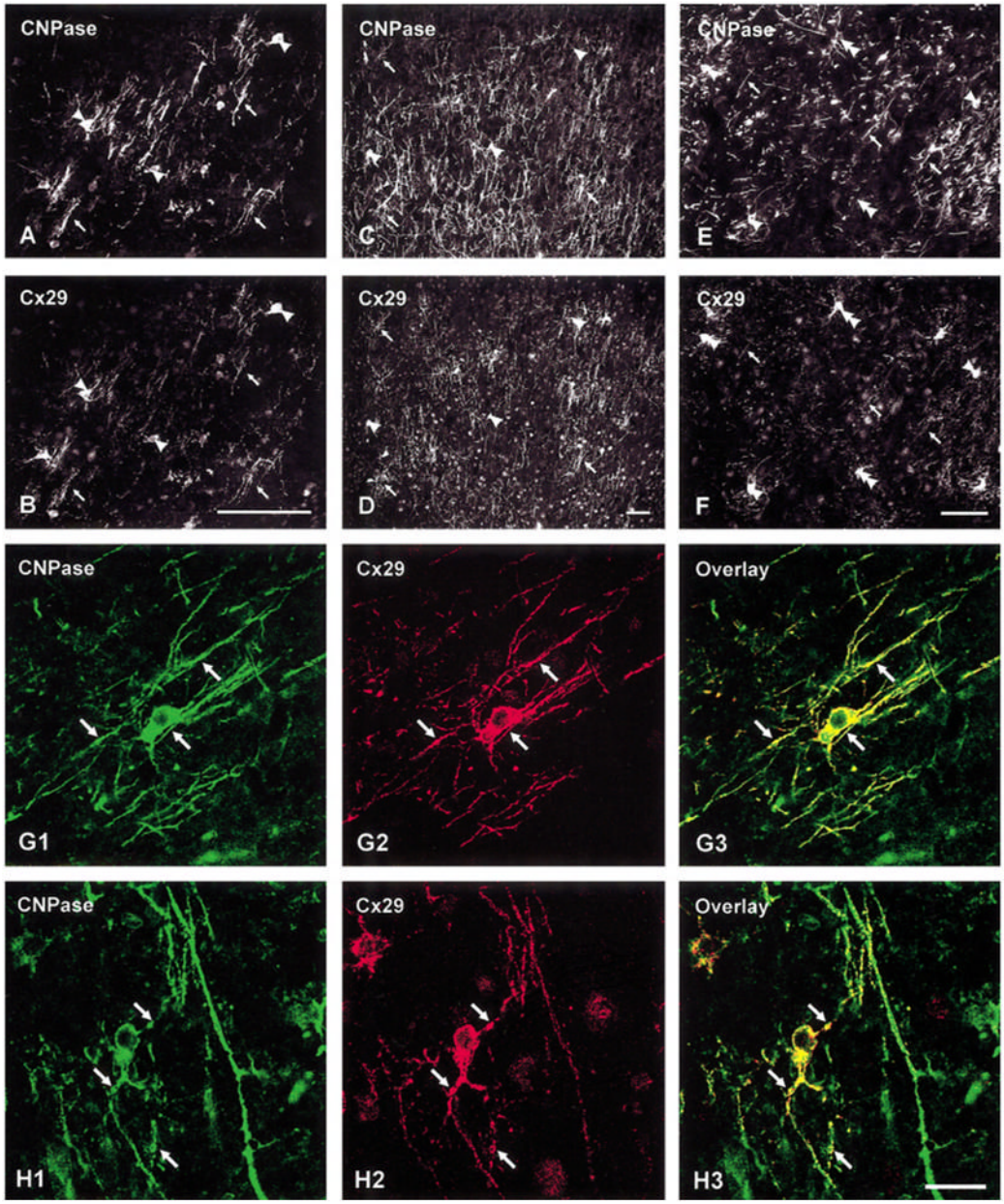

Fig. 4.

Immunofluorescence micrographs illustrating developmental profiles of Cx29. **A,B:** Double labeling in a field of corpus callosum at postnatal day 8 showing CNPase-positive fibers (A, arrows) and oligodendrocyte somata (A, arrowheads) labeled for Cx29 (B). **C–F:** Double labeling for CNPase (C,E) and Cx29 (D,F) in a field of cerebral cortex (C,D) at postnatal day 14 and in the hypothalamus (E,F) at postnatal day 20. CNPase-positive fibers are sparsely labeled for Cx29 (arrows), whereas oligodendrocyte cell bodies (arrowheads) are intensely labeled for Cx29, but occasionally exhibit weak labeling for CNPase (E, double arrowheads). **G,H:** Confocal double immuno-fluorescence of fields in the cerebral cortex at postnatal day 14 showing colocalization of labeling for CNPase (**G1,H1**) and Cx29 (**G2,H2**) around an oligodendrocyte (G, arrows) and several Cx29-positive processes emanating from a Cx29-

positive oligodendrocyte somata (H, arrows). **G3, H3:** Overlays. CNPase, 2,′3′-cyclic nucleotide 3′-phos-phodiesterase; Cx, connexin. Scale bars = 100 μm in A–F, 20 μm in G,H.

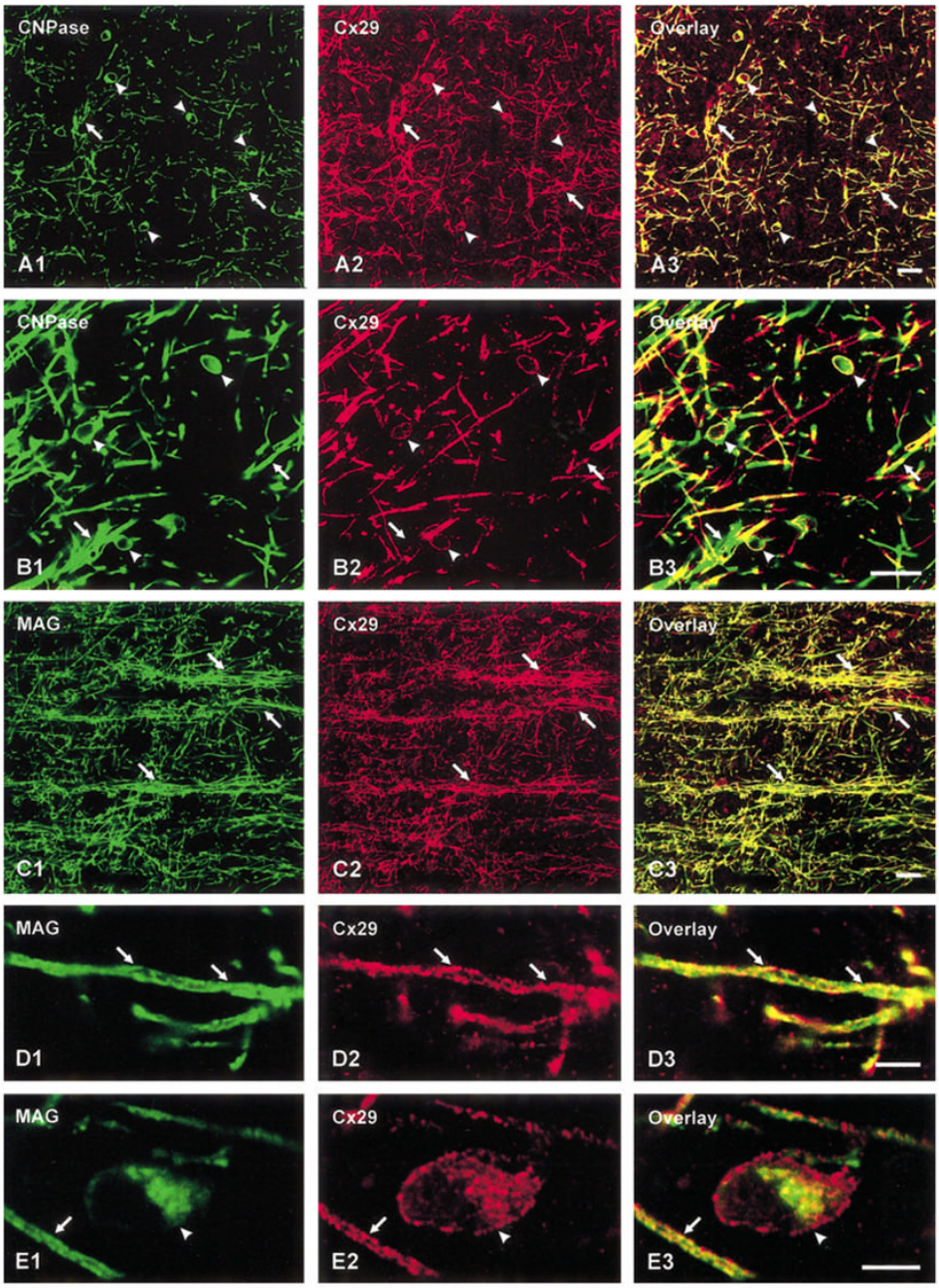

Fig. 5.

Confocal immunofluorescence showing association of Cx29 with the oligodendrocyte markers CNPase and MAG. **A,B:** Fields in the ventral anterior thalamic nucleus (**A**) and the cerebral cortex (**B**) double labeled for CNPase (**A1,B1**) and Cx29 (**A2,B2**). CNPase-positive fibers (arrows) and oligodendrocyte cell bodies (arrowheads) are immunopositive for Cx29 (yellow in image overlays, **A3,B3**). **C–E:** The same fields (**C1,C2; D1,D2; and E1,E2**) in the cerebral cortex double-labeled for MAG and Cx29, as indicated. Low and high magnifications show substantial colocalization of MAG and Cx29 along myelinated fibers (arrows) and partial colocalization in oligodendrocyte somata (E, arrowhead) as shown by yellow in image overlays

(**C3,D3,E3**). Cx, connexin; MAG, myelin-associated glycoprotein. Scale bars = 20 μm in A–C, 2.5 μm in D,E.

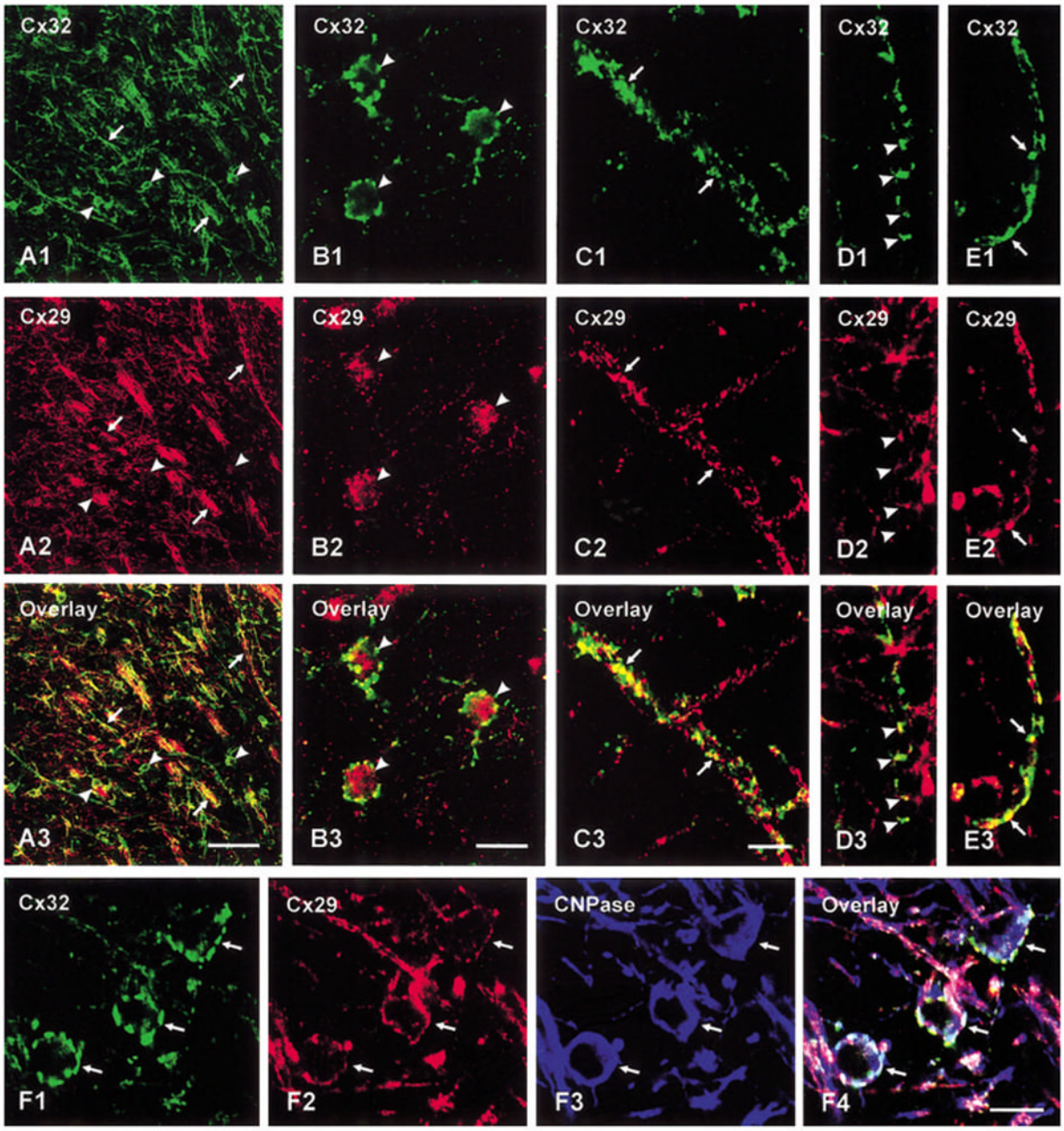

Fig. 6.

Confocal immunofluorescence colocalization of Cx29 with Cx32 in the adult brain. Each column of images in A to E illustrates a field double labeled for Cx32 (green) and Cx29 (red), with colocalization appearing as yellow in image overlays. **A:** Low magnification in a field of thalamus showing Cx32 colocalization with Cx29 along myelinated fibers (arrows) and oligodendrocyte cell bodies (arrowheads). **B:** Oligodendrocyte somata in the thalamus displaying punctate labeling for Cx32 (**B1,** arrowheads), finer punctate labeling for Cx29 intracellularly and at the cell periphery (**B2,** arrowheads), and partial colocalization of the two connexins (**B3**). **C–E:** Labeling for Cx32 and Cx29 along myelinated fibers in the cerebral cortex (C,D) and thalamus (E) appears as puncta (C,E, arrows) or intermittent strands (D, arrowheads), which exhibit partial colocalization (**C3,D3,E3**). **F:** Confocal triple

immunofluorescence showing that cells immunolabeled for Cx32 (**F1,** arrows) and Cx29 (**F2,** arrows) are CNPase positive (**F3,** arrows), as seen in overlay of images (**F4**). CNPase, 2,′ 3′-cyclic nucleotide 3′-phosphodiesterase; Cx, connexin. Scale bars = 20 μm in A, 10 μm in B, 5 μm in C3 for C–E, 5 μm in F.

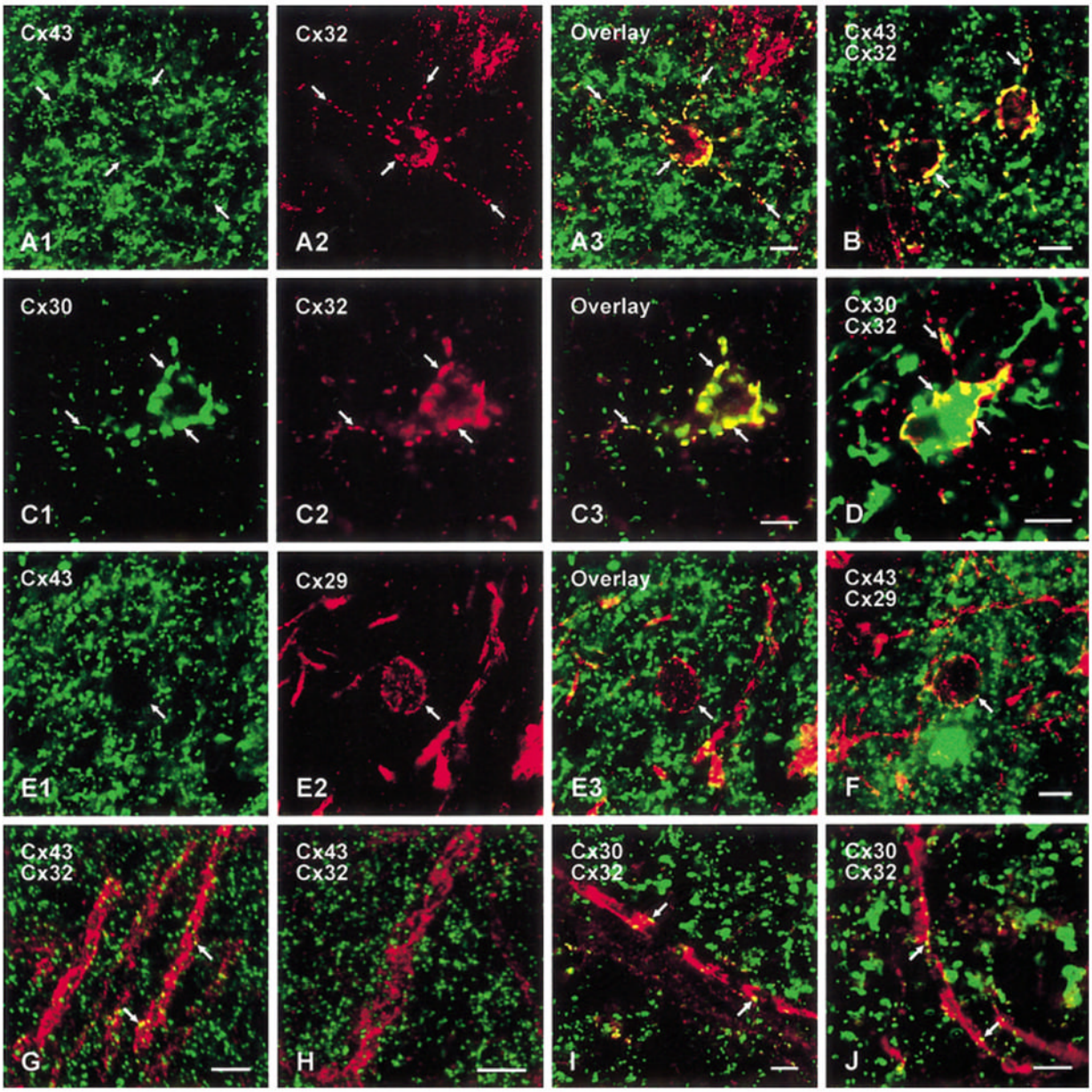

Fig. 7.

A–C: Confocal double immunofluorescence of Cx43 and Cx30 with Cx32 in the adult brain. In fields of the hypothalamus (A) and thalamus (B; shown only by overlay), some Cx43-positive puncta are co-associated with Cx32 on oligodendrocytes and their initial processes (A,B, arrows). In a field of cerebral cortex (C), intense punctate labeling for Cx30 (**C1,** arrows) is co-associated with Cx32 (**C2,** arrows) on oligodendrocyte somata (**C3,** overlay). **D:** Confocal double labeling showing Cx30 association with CNPase-positive oligodendrocyte in the cerebral cortex (arrows) as seen by yellow in the overlay. **E,F:** Confocal double labeling of Cx43 and Cx29 in adult brain. In fields of globus pallidus (E) and hypothalamus (F; shown only by overlay), minimal co-association of Cx43-positive puncta is seen with Cx29 on oligodendrocyte somata (arrows). **G–J:** Confocal double immunofluorescence labeling of astrocytic Cx43 (green) and Cx30 (green) in relation to labeling of Cx32 (red) along myelinated

fibers. Overlay images of fields in cerebral cortex (G) and thalamus (H) show limited co-association of Cx43-positive puncta with Cx32-positive fibers (arrows). Overlay images of fields in thalamus (I) and habenula (J) show sparse co-association of Cx30-positive puncta with Cx32 along fibers (arrows). CNPase, 2,′3′-cyclic nucleotide 3′-phosphodiesterase; Cx, connexin. Scale bars = 5 μm.

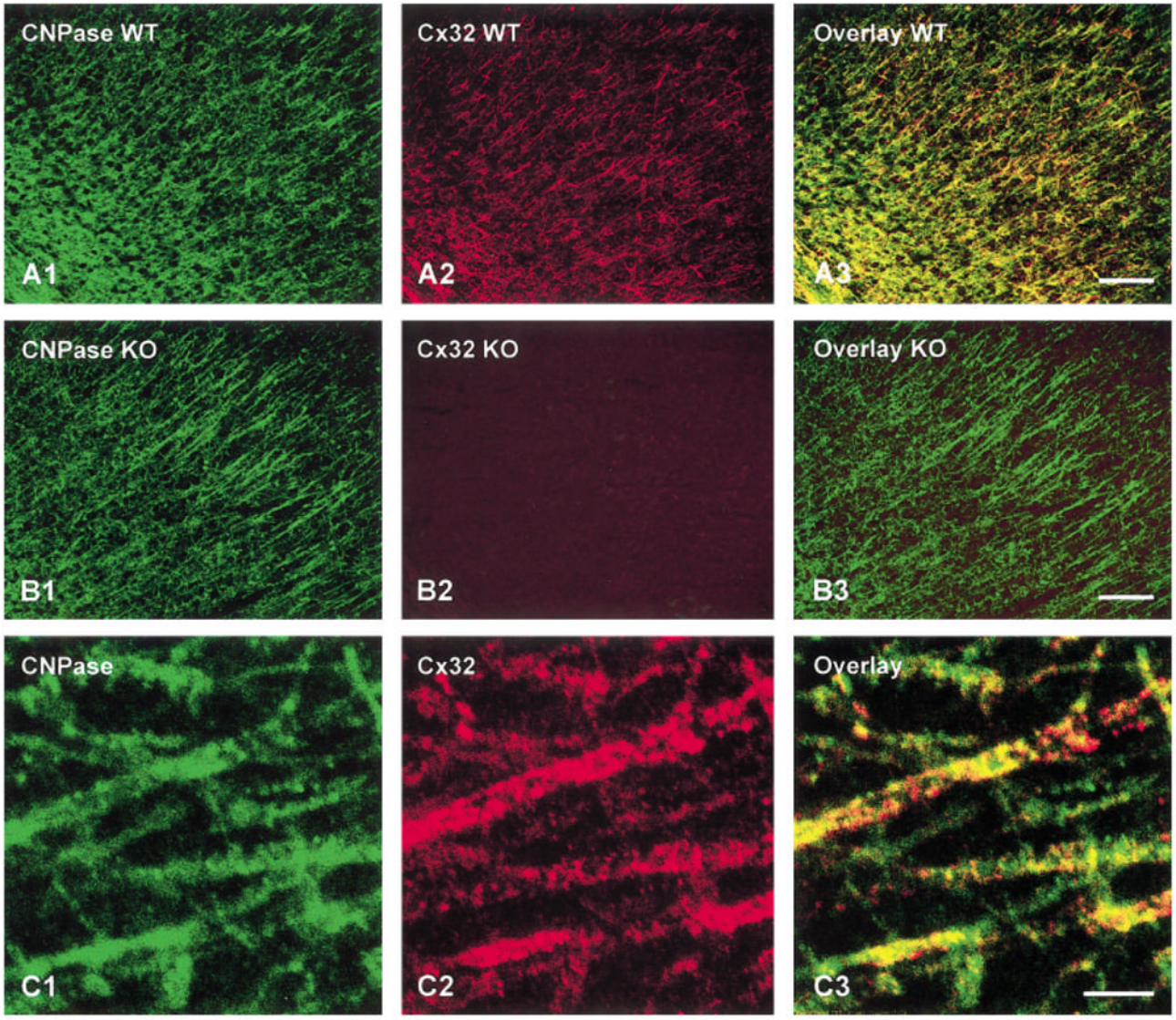

Fig. 8.

Immunofluorescence micrographs of Cx32 associated with myelinated fibers in the mouse cerebral cortex. **A:** Low magnification of a cortical field from a WT mouse double labeled for CNPase (**A1**) and Cx32 (**A2**), with colocalization shown in the overlay (yellow in **A3**). **B:** A cortical field from a Cx32 KO mouse double labeled for CNPase (**B1**) and Cx32 (**B2**) showing absence of Cx32 with consequent absence of yellow in the overlay (**B3**). **C:** Confocal double immunofluorescence of a field in a WT mouse showing CNPase-positive fibers (**C1**) labeled for Cx32 (**C2**) as seen by the overlay (**C3**). CNPase, 2,′3′-cyclic nucleotide 3′-phosphodiesterase; Cx, connexin; KO, knowckout; WT, wild type. Scale bars = 200 μm in A,B, 5 μm in C.

TABLE 1

Connexin Antibodies Used for Western Blotting and Immunohistochemistry

Antibody	Type[1]	Epitope; designation	Dilution	Reference; source
Cx29	Polyclonal	C terminus; 34-4200	0.6 μg/ml	Li et al., 2002; Zymed
Cx30	Polyclonal	C terminus; 71-2200	2.5 μg/ml	Nagy et al., 1999; Zymed
Cx32	Monoclonal	aa 235-246; 7C7	1:25	Li et al., 1997
Cx32	Monoclonal	C terminus; 35-8900	1 μg/ml	Zymed
Cx32	Polyclonal	Cytoplasmic loop; 71-0600	1.25 μg/ml	Li et al., 1997; Zymed
Cx32	Polyclonal	C terminus; 34-5700	2.5 μg/ml	Zymed
Cx32	Polyclonal	C terminus; sc-7258	2 μg/ml	Santa Cruz Biotech
Cx43	Monoclonal	C terminus; 35-5000	3.5 μg/ml	Zymed
Cx43	Polyclonal	C terminus; 71-0700	0.25 μg/ml	Li et al., 1998; Zymed
Cx43	Monoclonal	aa 252–270; mAb 3067	2 μg/ml	Chemicon
Cx43	Polyclonal	aa 346–363; 18A	1:1,000	Yamamoto et al., 1990a,b

[1] All monoclonal antibodies were raised in mouse. All polyclonal antibodies were raised in rabbit, except polyclonal anti-Cx32 sc-7258, which was raised in goat. Cx, connexin; mAb, monoclonal antibody.